Nonlinear electrodynamics in the granular superconductor $YBa_2Cu_3O_7$: Experiments and interpretation

C. D. Jeffries, Q. H. Lam, Y. Kim, C. M. Kim, and A. Zettl
Physics Department, University of California, Berkeley, California 94720
and Materials and Chemical Sciences Division, Lawrence Berkeley Laboratory, Berkeley, California 94720

M. P. Klein
Calvin Laboratory, Lawrence Berkeley Laboratory, Berkeley, California 94720
(Received 23 January 1989)

For bulk samples of superconducting $YBa_2Cu_3O_7$ powder and pellets subject to a dc magnetic field H_0 and a parallel ac magnetic field H_1 at frequency $f \sim 10^3$ to 10^5 Hz, we report data on the generated harmonic power $P(nf)$ up to harmonic $n \approx 40$, finding: (1) If $H_0 = 0$, only odd harmonics; (2) if $H_0 \neq 0$, even harmonics are additionally generated; (3) for H_1 sufficiently large ($\gtrsim 10$ Oe) and n large, then $P(nf)$ vs H_0 displays sharp and deep periodic dips, revealing a remarkably consistent and reproducible macroscopic flux quantization for the bulk sample. These data, as well as the relative intensities of the harmonic power, are found to be in semiquantitative agreement with detailed numerical predictions of a dynamical model of the material as a suitably averaged ensemble of prototype flux quantized loops with weak links. At lower values of H_1 additional structure is observed, related to fluxon pinning and depinning.

I. INTRODUCTION

Soon after the discovery of the superconducting copper oxides, the ceramic specimens were found to be granular with weak links, having properties[1] somewhat like those predicted for superconducting glass clusters.[2] Some unusual properties reported for bulk $YBa_2Cu_3O_7$ (Y-Ba-Cu-O) were strong dependence of ac susceptibility on the magnitude of the ac field;[3,4] nonresonant microwave absorption in very low magnetic fields ($H \sim 10$ Oe);[5] sharp decrease in transport critical current in low magnetic fields;[6] and limited critical current in high magnetic fields. Novel nonlinear electrodynamics has been reported[7] including extensive harmonic generation which could be semiquantitatively understood by modeling the system as a suitably averaged collection of flux-quantized supercurrent loops containing Josephson junctions. In an extension[8] of this model we have predicted that the harmonic power will show strikingly sharp dips periodic in the dc field, even with broad distributions of loop areas and orientations, e.g., as in sintered, polycrystalline, or powdered samples. One would have naively expected the periodic flux quantization of the prototype loops to be averaged out, but this is not predicted for high harmonics. The present paper presents detailed experimental results on Y-Ba-Cu-O, many of which are in semiquantative agreement with the model predictions. Similar results will be separately reported for $Bi_4Sr_3Ca_3Cu_4O_x$.[9] In Sec. II we describe the apparatus, procedures, and samples used. Section III briefly reviews the theoretical model.[7,8] The data are presented in Sec. IV and compared to the predictions of the model. Section V summarizes the results and suggests further work on the rather complex problem of understanding the electrodynamics of these granular materials.

II. EXPERIMENTAL PROCEDURE

The method we used to study nonlinear electrodynamical behavior consists essentially of observing and processing the voltage induced into a copper "receiver" coil wound around a Y-Ba-Cu-O sample, subject to applied dc and ac magnetic fields. More specifically, the data shown in this paper were obtained as follows. A sample of cylindrical proportions is subject to three applied magnetic fields, all uniform and coaxial: (i) an ac field $H_1(t) = H_1 \sin\omega t$, with $0 < H_1 < 23$ Oe, and frequency $f = \omega/2\pi \approx 10^2$ to 10^6 Hz; (ii) a dc field H_0, $0 < H_0 < 100$ Oe; (iii) a repetitive "scan" field $H_s(t)$ of triangular waveform at a low frequency $\approx 10^{-2}$ Hz. These fields were produced by copper solenoids immersed in liquid N_2 in a magnetically shielded Dewar. Solenoids (i) and (iii) were driven by very stable, independent synthesized function generators (HP model 3325A). Two arrangements of sample and receiver coils were used: (a) in the "two-coil" method, a long cylindrical sample (2.7×10 mm^2) of powdered Y-Ba-Cu-O sealed in a quartz tube (sample "C-15") is located in a 4-mm-diameter solenoid in series with an identical but empty counterwound solenoid. Except for the last figure, all data were taken by this two-coil method, using this sample.[10] (b) A rectangular bar ($2 \times 2 \times 9$ mm^3) of sintered Y-Ba-Cu-O [sample "C-40" (Ref. 11)] with $T_c = 91$ K, closely wound with a single receiver coil of 27 turns of 36 gauge copper wire. Both the one-coil and the two-coil methods yield a signal voltage of the form

$$V_{sn}(t) = A_n \sin(n\omega t) + B_n \cos(n\omega t), \quad n = 1,2,\ldots, \qquad (1)$$

which is processed by an analog spectrum analyzer with a 90-dB dynamic range (HP model 3585A), to yield the power spectral components $P(nf) \propto (A_n^2 + B_n^2)$. However,

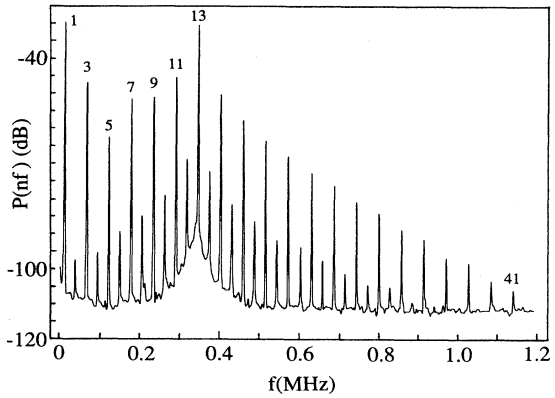

FIG. 1. Power spectrum for powdered Y-Ba-Cu-O (sample C-15) at $T=77$ K, driven by an ac field at $f=28$ kHz, of amplitude $H_1=23$ Oe, in a dc field $H_0\approx 1$ mOe. Odd harmonics up to $n=41$ are clearly observed, as well as much weaker even harmonics. The broad background resonance at $f\approx 363$ kHz is that of the receiver coil itself.

the two-coil method allows a balancing out of the fundamental component ($n=1$), giving improved sensitivity to the high harmonics; harmonics up to $n\approx 41$ can be readily observed (see Fig. 1). We study and report here $P(nf)$ as a function of the parameters H_0, H_1, f, n and the temperature T of the sample.

The signal $V_{sn}(t)$ is also processed, for $n=1$ and 2, by a phase-sensitive lock-in detector (PARC model 5209), with output voltage V_c. For $n=1$ and assuming linear susceptibility theory for the sample magnetization,

$$M=\chi' H_1\sin\omega t+\chi'' H_1\cos\omega t\ ,$$

where χ' and χ'' are the real and imaginary components of the complex ac susceptibility $\tilde{\chi}\equiv\chi'-i\chi''$, one can define a normalized output voltage proportional to

$$V_c/H_1\propto(1+4\pi\chi')\ \text{ or }\ (-4\pi\chi'')\ ,$$

respectively, for the in-phase and in-quadrature components of the lock-in output voltage, for the one-coil method. For the two-coil method one finds $V_c/H_1\propto(4\pi\chi')$ or $(-4\pi\chi'')$, respectively. Here, for simplicity in expression, we have neglected the demagnetization effect in the sample, which will be taken into account later in actual calculation of χ'. In this paper our primary concern is with the harmonics rather than the linear susceptibility.

All data shown were taken with the sample cooled in "zero" dc field ($H_0\lesssim 1$ mOe) by immersion in liquid nitrogen. Essentially similar results were obtained in a variety of ceramic pellets and powdered Y-Ba-Cu-O samples; the general features are believed to be generic. We only show data for $f=28$ to 52 kHz; the results are not very sensitive to frequency in this range.

III. MODEL

Since details of our model have been given in previous papers,[7,8] we will only briefly review it here and summarize some of the equations of its different versions for use in numerical evaluations to be compared to the experimental data in Sec. IV.

The granular superconducting sample, in the presence of magnetic fields, is assumed to be essentially composed of a collection of current loops formed by superconducting "grains" in contact through Josephson junctions or other weak links. We model these loops, complex as they may physically be, by a simple prototype resembling an rf SQUID (superconducting quantum interference device), a thin ring-shaped loop of area S_0 in series with a single junction. In our model, these loops are assumed not to be coupled and to behave independently from one another. We then study the behavior of the signal one would get from the surrounding receiver coil if an ensemble of these prototype loops of various areas and orientations is driven by an applied ac magnetic field superposed on an applied dc field. All loops are assumed to be subject to the same external fields. In our model, the areas of the junctions are assumed to be much smaller than the loop areas, so that the diffractionlike pattern of the junction as a function of dc field can be neglected at low fields. Then the Josephson current-phase relation becomes

$$I(t)=I_c\sin\gamma\ ,$$

where I_c is the junction critical current, and the phase difference γ is proportional to the instantaneous number of flux quanta enclosed by the loop.

Zero-order model. In the simplest version of the model, we assume I_c to be small and neglect the field generated by the loop current itself and thus

$$\gamma=(2\pi S_0/\Phi_0)(H_0+H_1\sin\omega t)\ ,$$

where $\Phi_0=hc/2e$ is the flux quantum, and the quantity in the second set of parentheses is the total applied field. Due to the nonlinearity of the current-phase relation, harmonics will be generated in the loop current and should be detected by the receiver coil. Define the dimensionless quantities

$$\alpha\equiv 2\pi S_0 H_0/\Phi_0,\quad \beta\equiv 2\pi S_0 H_1/\Phi_0\ ,$$

where S_0 is a characteristic loop area, and $\alpha/2\pi$ is just the number of flux quanta in the loop due to H_0, etc. For a single loop the Fourier components of the current are

$$I_n(t)\propto J_n(\beta)\sin\alpha\cos(n\omega t),\quad n\ \text{even}\ ,$$

$$I_n(t)\propto J_n(\beta)\cos\alpha\sin(n\omega t),\quad n\ \text{odd}\ ,$$

where $J_n(\beta)$ is the Bessel function of integer order n. Assume that in a particular ensemble the loop areas S are characterized by a distribution function $F(A)$, with $A\equiv S/S_0$. Then, integrating over all the loops, the signal amplitude of the nth harmonic as detected by the receiver coil should be

$$\langle V_n\rangle=n\omega\int_{A=\delta}^{\infty}AJ_n(A\beta)\cos(A\alpha)F(A)dA/G,\quad \text{odd}\ n\ , \tag{2a}$$

$$\langle V_n\rangle=n\omega\int_{A=\delta}^{\infty}AJ_n(A\beta)\sin(A\alpha)F(A)dA/G,\quad \text{even}\ n\ , \tag{2b}$$

where

$$G=\int_{A=\delta}^{\infty}F(A)dA\,,$$

and $\delta>0$ is a lower cutoff. We have shown numerically[8] that loop orientations may be approximately neglected in Eq. (2). In this model the signal has only one phase and the harmonic power is $P(nf)=20\log_{10}|\langle V_n\rangle|$ dB.

Loop model. Another version of the model explores the possibility that the current-flux relation of the prototype loop is not sinusoidal, but still periodic with period Φ_0. We name this version as such because one of many possible reasons for a nonsinusoidal, periodic current-flux relation is that there may be current loops in the sample which simply do not have junctions in their paths, and obey London's fluxoid quantization equation. In that particular case the current-flux relation is a sawtooth function, and the Fourier series of such a function is given by

$$I(t)=\sum_{m=1}^{\infty}(-1)^{m+1}m^{-1}\sin(m2\pi\Phi/\Phi_0)\,.$$

For convergence we will arbitrarily replace the coefficients $1/m$ above by $\exp(-m+1)$ to somewhat smooth the sawtooth. The sample-averaged harmonic signal components for this model version are then

$$\langle V_n\rangle=n\omega\sum_{m=1}^{\infty}(-1)^{m+1}e^{-m+1}\times\int_{A=\delta}^{\infty}AJ_n(mA\beta)\cos(mA\alpha)F(A)dA/G\,, \tag{3}$$

for odd n. Again, $\cos(mA\alpha)$ is to be replaced by $\sin(mA\alpha)$ for even n. Also, orientation averaging has been neglected.

First-order model. In order to take the self-field and dissipation of any normal current component into account, we introduce a self-inductance L to the loop and shunt the junction by a resistance R. The self-inductance produces a field LI which opposes the external field, causing screening. Thus a relaxation time to the loop current, $\tau\approx L/R$, is also introduced. A first-order nonlinear differential equation describing the loop current in response to the ac field is then derived to be

$$\omega^{-1}\frac{dI_1}{dt}=(\kappa L_0)^{-1}[\sin(\alpha+\beta\sin\omega t-L_0I_1)-I_1]+\left[\frac{\beta}{L_0}\right]\cos\omega t\,, \tag{4}$$

where $I_1\equiv I/I_c$, $\kappa\equiv\hbar\omega/2eRI_c$, $L_0\equiv 2\pi LI_c/\Phi_0$. The signal voltage of the receiver coil due to a prototype loop is proportional to dI_1/dt, computed by numerical iteration. By averaging over a distribution of loop areas $F(A)$ and Fourier transforming dI_1/dt numerically, we get the harmonic signals predicted by this model.

These three variations of the model predict similar but not exactly the same behavior. However, they all predict the following. (1) If $H_0=0$, then $\alpha=0$ and only odd harmonics are generated. (2) If $H_0\neq 0$, then even harmonics are additionally generated. These two conclusions arise from the symmetry in Eq. (2). (3) If H_1 is sufficiently large then the harmonic power $P(nf)$ for both even and odd n displays sharp, essentially periodic dips as dc field H_0 is scanned, revealing periodic flux quantization of the prototype loop, even in a "random" granular sample.

IV. EXPERIMENTAL RESULTS AND INTERPRETATION

It will become evident below that much of the data shows a nonlinear dependence on the ac field H_1 which allows one to distinguish a transition between several regions: a "high-H_1" region, roughly $2<H_1<25$ Oe, an intermediate region $0.2<H_1<2$ Oe, and a "low-H_1" region, roughly $10^{-3}<H_1<0.2$ Oe, although there is *not always a clear distinction.* We first show some data in the high-H_1 region.

Extensive harmonic generation. Figure 1 shows the harmonic power $P(nf)$ versus the harmonic number n for Y-Ba-Cu-O powder sample C-15 at $T=77$ K, taken by the two-coil method, with $H_1=23$ Oe, $H_0\approx 1$ mOe. The power falls off slowly with n; all odd harmonics up to at least $n=41$ are clearly observed, superposed on a broad receiver coil resonance at 363 kHz.

Figure 2 shows the $P(nf)$ vs n data of Fig. 1, corrected for the receiver coil resonance; the slope for large n is 1.9 dB/harmonic. The broken line is that computed for the zero-order model, Eq. (2a) with the area distribution

$$F(A)=\sinh(A\pi/2)/[A(\cosh(A\pi)-1)]\,, \tag{5}$$

which is to be discussed below; the slope for large n is 2.4 dB/harmonic; this model thus gives a reasonable explanation of the slow falloff of the harmonic power. The dotted line, computed for the first-order model, Eq. (4), does not fit the data owing to a resonance near $n=17$ due to the choice of the parameters L_0 and κ.

Plots of $P(nf)$ vs H_1 for $n=3$, 5, and 7 show a roughly cubic dependence on H_1 in the intermediate-H_1 region,

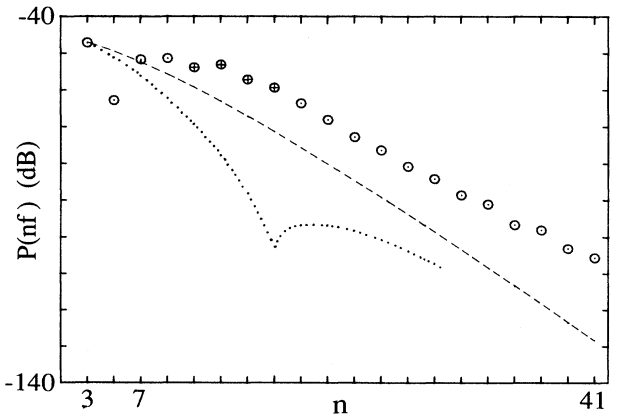

FIG. 2. Circles: $P(nf)$ vs harmonic number n from Fig. 1; crossed circles: data from Fig. 1 corrected for receiver coil resonance. Broken line: relative $P(nf)$ computed from the model Eqs. (2) and (5), $\beta=5$, adjusted to fit data at $n=3$. Dotted line: $P(nf)$ computed for first-order model, Eq. (4), with $\beta=5$, $L_0=0.35$, $\kappa=0.3$, as in Fig. 8.

for which we have no numerical model, and more complex behavior in the high-H_1 region. We note that Xia and Stroud[12] have developed a model of superconducting clusters by which they try to explain the power dependence on n reported earlier.[7]

Temperature dependence. The circles in Fig. 3 show the temperature dependence of $P(2f)$ at $H_0=2.7$ Oe and $H_1=2.3$ Oe, i.e., in the high-H_1 region. Order harmonics show quite similar behavior. The solid line is a fit of the Ambegaokar-Baratoff expression[13] for the critical current of a Josephson junction

$$J_c=[\pi\Delta(T)/2eR_n]\tanh[\Delta(T)/2kT]\,, \qquad (6)$$

where we have used the high-temperature limit for the gap $\Delta(T)/\Delta(0)=1.74(1-T/T_c)^{1/2}$ with $T_c=88.5$ K, chosen for best fit. Although there are fluctuations at $T_c\pm 2$ K, the data fit this expression over 3 orders of magnitude, but only for our limited temperature range, T_c to 77 K. This suggests that the weak links are Josephson junctions, but other types of weak links cannot be ruled out.

Symmetry of harmonic power. Figure 4(a) shows the second harmonic power $P(2f)$ as a function of H_0, obtained by slowly scanning from $H_0=+20$ to -20 Oe. The dip at $H_0=0$, shown in expanded scale in Fig. 4(b), is very narrow, $\Delta H\sim 0.1$ mOe; $P(2f)$ increases by 85 dB for a dc field change of ~ 1 Oe. This is qualitatively in agreement with the prediction of the model, based on the symmetry of Eq. (2b), that $P(nf)\rightarrow 0$ as $H_0\rightarrow 0$ for even n. To observe this very narrow dip it is necessary to both use $H_1\gtrsim 2$ Oe and to cool in zero field to reduce the remnant local fields due to pinned fluxons. Moreover, there is some experimental evidence that this very narrow dip is an unstable state. If the dc field is scanned up to $H_0>5$ Oe and back, the narrow dip cannot be recovered without zero field cooling, possibly the result of pinned fluxons. The system appears to be somewhat unstable, probably at localized sites, against self-symmetry-breaking.

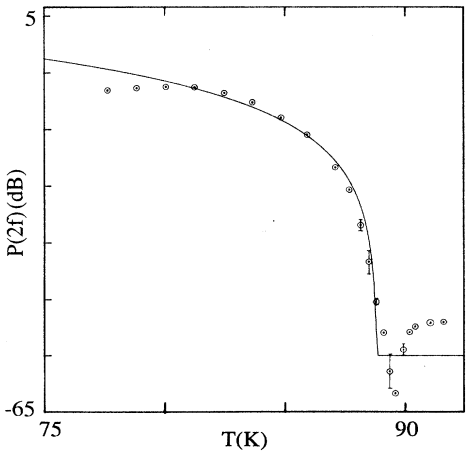

FIG. 3. Circles: observed intensity of $P(2f)$ vs temperature T for Y-Ba-Cu-O powder, sample C-15 with $f=52.5$ kHz, $H_0=2.7$ Oe, $H_1=2.3$ Oe. Solid line: computed behavior from Eq. (6).

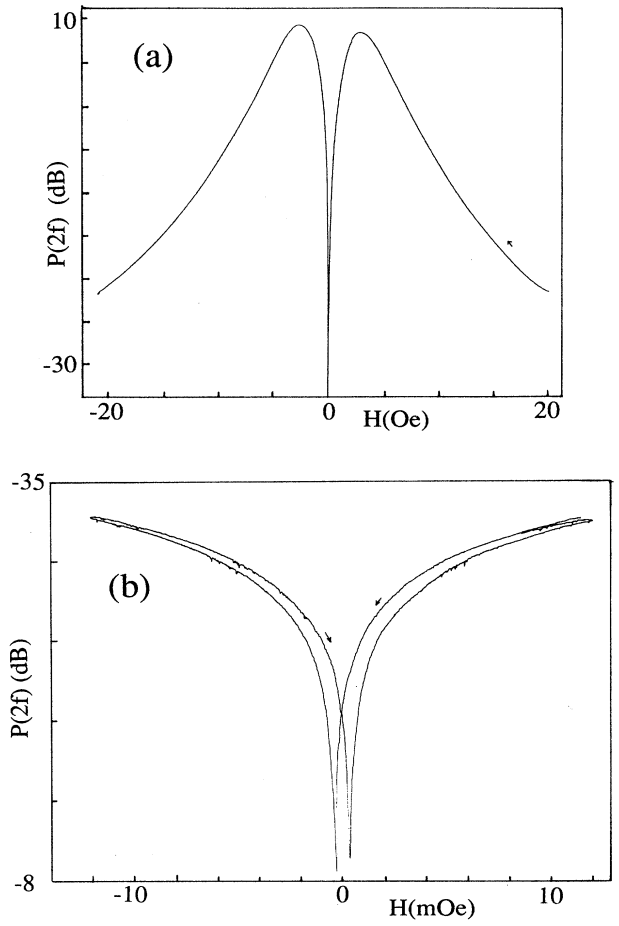

FIG. 4. (a) Second harmonic power $P(2f)$ vs dc field H_0 for Y-Ba-Cu-O (sample C-15) at $T=77$ K, $H_1=2.3$ Oe, $f=52.5$ kHz. (b) Expansion of the scan resolution by 2000×, showing narrow dip at $H_0=0$, of width $\Delta H_0\sim 0.1$ mOe.

Flux quantization. Yet another aspect of the nonlinear electrodynamics observable in Y-Ba-Cu-O powder is shown in Fig. 5, the relative harmonic power for selected harmonics, versus H_0, scanned at a uniform rate for field increasing and then decreasing; the ac field has the relatively large value $H_1=23$ Oe. For $n=2$ the trace is similar to Fig. 4 except for a broader dip at zero field and a larger hysteresis. However, for the higher harmonics, both even and odd, a series of sharp dips is observed, approximately equally spaced, with average spacing ΔH_0 inversely proportional to n. These dips are distinct evidence for flux quantization of superconducting loops in the granular sample and are a confirmation of the predictions of the model in Sec. III. For example, Fig. 6 shows $P(nf)$ vs α, computed for the zero-order model, Eqs. (2) and (5), for the same harmonics as Fig. 5. Since α is just proportional to H_0 a strong correspondence between experiment and model is readily apparent for all harmonics. The small hysteresis in the data is believed to have an origin in pinning and depinning of fluxons, as discussed by Blazey *et al.*[14]

In the computation for Fig. 6 we used the loop area dis-

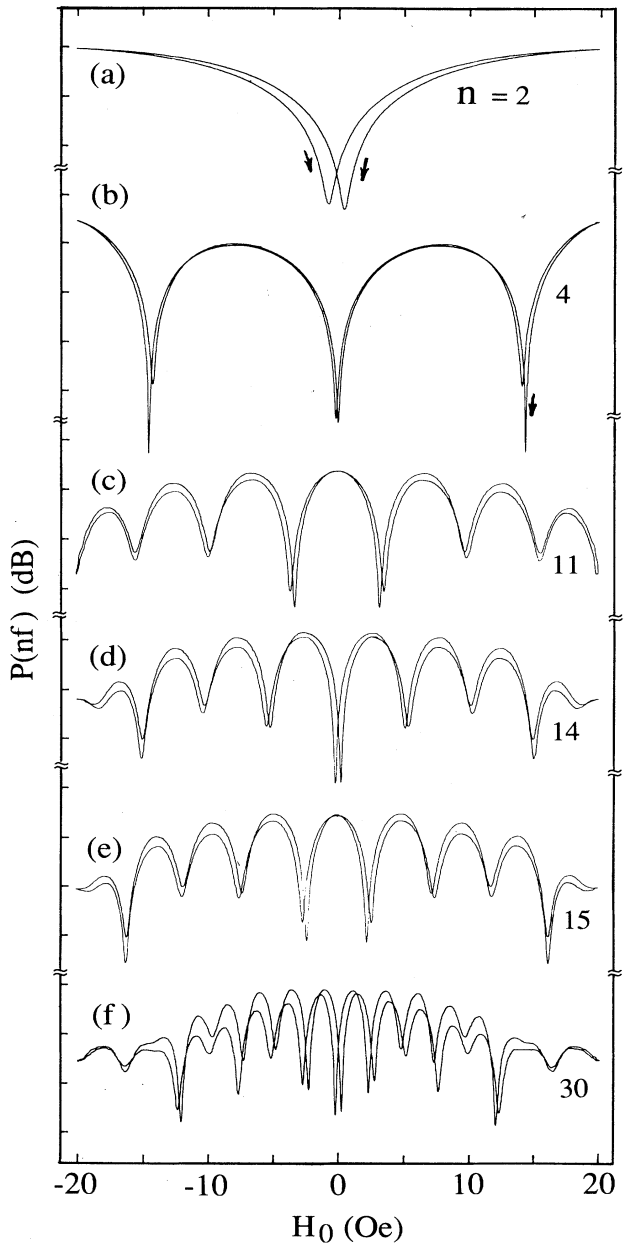

FIG. 5. Relative harmonic power (10 dB/div) of $P(nf)$ vs H_0, scanned at a uniform rate, for sample C-15, powdered Y-Ba-Cu-O, at $T=77$ K, $f=28$ kHz, $H_1=23$Oe. (a) to (f) show data for selected representative harmonics n. Shown are two scans, the arrows denoting the direction of time increase. There is a small hysteresis with this property: if a leftward trace is reversed, it superposes exactly on the rightward trace. The sharp dips are a consequence of flux quantization of an ensemble of supercurrent loops in the granular sample.

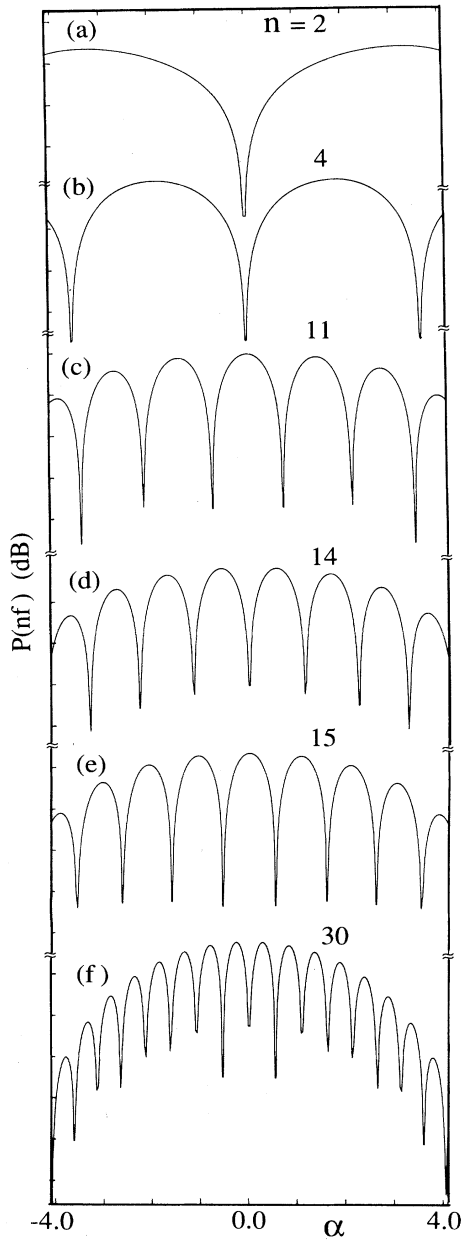

FIG. 6. Relative harmonic power (10 dB/div) of $P(nf)$ vs α, computed from zero-order model Eq. (2), using $\beta=5$ and $F(A)$ from Eq. (5). (a) to (f) show the same harmonic numbers as for the data, Fig. 5.

tribution function Eq. (5). This monotonically decreasing expression was not chosen arbitrarily, but rather empirically, in order to yield from the integral in Eq. (2b), for $n=0$, a dc magnetization of the form $M(H_0)\sim\tanh(H_0/H_{01})$, which is an *approximate* representation of the low-field data reported[6,15] for granular Y-Ba-Cu-O at 77 K for which $H_{01}\sim 10$ Oe. Equation (2) was numerically integrated, with Eq. (5), and with limits of integration chosen as $\delta=0.005$ and $A_{\max}=30.0$. Even though Eq. (5) is singular at $A=0$, it was found that these limits yielded a magnetization within a few percent of the hyperbolic tangent function. Furthermore, we only use Eqs. (2) and (5) to compare the *relative* power for various harmonics, or, for a given n, variation of the harmonic signal with α; these results are not sensitive to the limits of integration as long as the singularity at $A=0$ is avoided. Equation (2) with Eq. (5) also qualitatively predicts the observed

shapes of the lock-in voltage signals V_c vs H_0, for $n=1$ and 2, and the falloff of $P(2f)$ in Fig. 4(a), as H_0 moves away from zero. Note that in Fig. 4(a) of Ref. 7, we explained the falloff by averaging the diffraction pattern of Josephson junctions. We now believe, however, that the falloff may eventually be explicable purely by a more carefully determined distribution function $F(A)$ which fits the data more quantitatively, without invoking the Josephson junction area as an additional parameter.

We also used Eq. (2) to compute $P(nf)$ vs α for the Gaussian distribution function

$$F(A)=\exp[-(A-1)^2/2\sigma^2], \tag{7}$$

finding predictions similar to Eq. (5) for large n [see, e.g., Fig. 1(c) of Ref. 8]. However, for small n, predictions do not agree well with experiment. From data like that of Fig. 5 we plot in Fig. 7(a) the average spacing ΔH_0 between dips for $n=3,4,\ldots,30$. Except for small n the data are well fit by the expression $\Delta H_0 \propto n^{-0.93}$. In similar fashion we compute from Eqs. (2) and (7) the average spacing $\Delta\alpha$, plotted in Fig. 7(b) for several values of the standard deviation σ of the Gaussian distribution. We find that the slope converges to -0.98 for $\sigma \gtrsim 2$. Using Eqs. (2) and (5), we also find a very good linear fit for $\Delta\alpha$ vs n with slope -0.97. So both calculation and experiment suggest that as n increases, the slope asymptotically approaches -1. We thus conclude that the decrease in spacing of the dips with n in Fig. 5 can be semiquantitatively understood by the zero-order model, and that it is not sensitively dependent on the assumed distribution function $F(A)$, other than that it should monotonically decrease for large A; however, Eq. (5) fits the data better than Eq. (7) for small n.

Figure 8 shows $P(nf)$ vs α computed from the first-order model, Eq. (4). This model provides a mechanism for dissipation, so it is not surprising that the dips are broader and less resolved, e.g., $n=15$ and 30. The Fourier transform of $\langle V_n(t)\rangle$ now contains both real and imaginary components, and both must vanish to give a deep power dip. The pattern is more complex, and, in fact, this feature is qualitatively observed, e.g., in Fig. 5(f), if we ignore the hysteresis. More work is being done on exploring the (L_0,κ) parameter space; values of L_0 and κ that fit the data quantitatively have yet to be found.

Why does a random sample show flux quantization? Recognizing that various versions of the model can explain the experimental finding of deep dips in the harmonic power, almost periodic in the dc field, we ask an in-

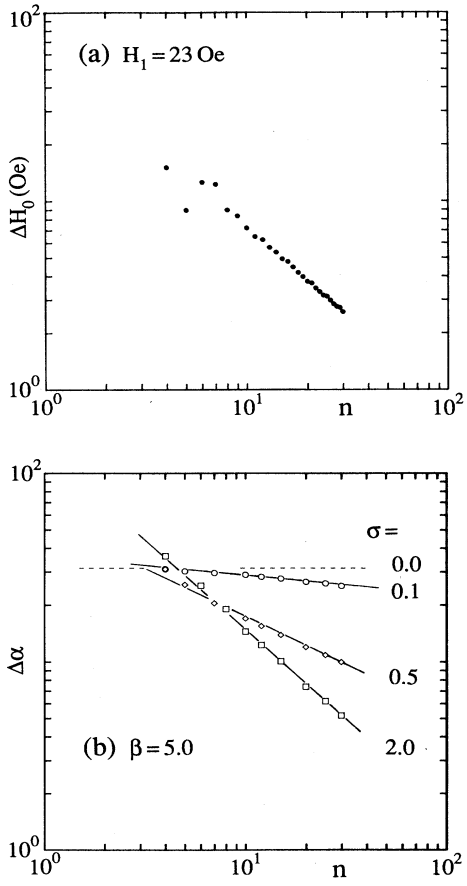

FIG. 7. (a) Average spacing ΔH_0 between dips from the data of Fig. 5, vs the harmonic number n. (b) Average spacing $\Delta\alpha$ between dips vs harmonic number n, computed from Eqs. (2) and (7) for various values of the standard deviation σ of the assumed Gaussian distribution.

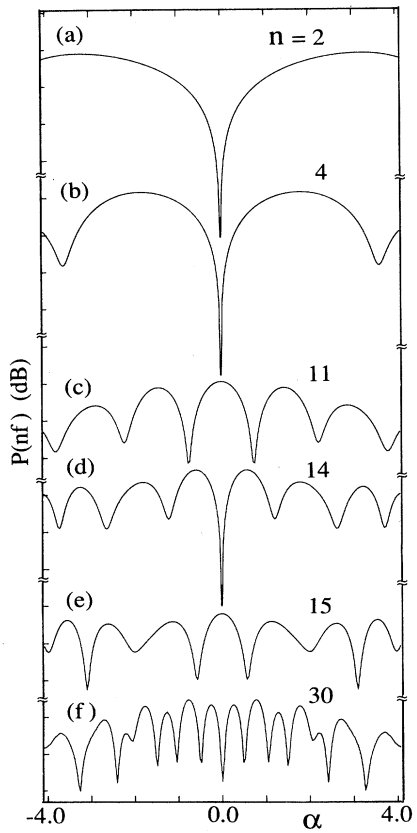

FIG. 8. Relative harmonic power (10 dB/div) of $P(nf)$ vs α, computed from the first-order model, Eq. (4), using parameters $\beta=5$, $L_0=0.35$, $\kappa=0.30$, and $F(A)$ from Eq. (5).

teresting question: How does it come about mathematically that all this structure is not averaged out in, say, Eq. (2). Or, to put the question in physical terms, why does a random powder sample of Y-Ba-Cu-O show sharp dips, e.g., as in Fig. 5(e), quite similar to those observed in fabricated thin film arrays of *identical* loops,[16] or arrays of *identical* junctions?[17] It will be easier to first answer this question mathematically by examining Eq. (2).

The general behavior of the voltage signal, as modeled by Eq. (2), is clearly determined by the integral in the equation. To understand the structure of the signal as a function of α, one can separate the integrand, say of Eq. (2a), into two factors: the periodic factor $\cos(A\alpha)$ and the amplitude $Q_n(\beta,A)\equiv AJ_n(A\beta)F(A)$. One recognizes that $Q_n(\beta,A)$ is, within a constant factor, the Fourier cosine transform of $\langle V_n(\alpha)\rangle$, for odd n; for even n, Eq. (2b), it is the sine transform. For $n\geq 1$, the Bessel function $J_n(x)$ initially increases rapidly as $J_n(x)\approx(x/2)^n/(n!)$, and then behaves like a damped oscillation. If the area distribution $F(A)$ is a sufficiently rapidly decreasing function, at least for large enough values of A, then $Q_n(\beta,A)$ will be a *rapidly decreasing oscillating function of A, with a well-defined peak at* $A^*_{n,\beta}$, dependent on n and β.

For example, in Fig. 9(a), we have used $F(A)$ from Eq. (5) and computed $|Q_n(\beta,A)|$ vs A for the parameters $n=10$ and $\beta=5.0$. It indeed shows successive decreasing peaks with the dominant peak at $A=A^*_{n,\beta}=2.09$, larger by a factor of 6.7 than the next peak. Thus the integral could roughly be evaluated at only the dominant value of A:

$$\langle V_{n,\beta}\rangle \sim A^*_{n,\beta}J_n(A^*_{n,\beta}\beta)F(A^*_{n,\beta})\sin(A^*_{n,\beta}\alpha)\,,$$

giving a harmonic power $P_n(\alpha)\sim\sin^2(A^*_{n,\beta}\alpha)$, with periodic spacing between dips $\Delta\alpha\approx\pi/A^*_{n,\beta}=1.50$, in good agreement with the directly calculated value of $\overline{\Delta\alpha}=1.52$ using the full expression equation (2b). To show the dependence on n, we plot, in Fig. 9(b), $|Q_n(\beta,A)|$ vs A for $n=5$, $\beta=5.0$, also using Eq. (5) for $F(A)$. In this case the location of the dominant peak decreases approximately by a factor of 2, to $A^*_{n,\beta}=1.10$, corresponding to dip spacing of $\Delta\alpha\approx\pi/A^*_{n,\beta}=2.86$, again in good agreement with $\overline{\Delta\alpha}=2.80$, directly calculated from Eq. (2a). Additional computation shows that $A^*_{n,\beta}$ is approximately proportional to n, in agreement with the full integral and also with the data, $\Delta H_n\propto n^{-1}$, as in Fig. 7, for large enough n.

One can take the view that $A^*_{n,\beta}$ is an "effective loop area" in the sense that the dip spacing $\Delta\alpha\propto(A^*_{n,\beta})^{-1}\propto n^{-1}$ is, for large n, determined by the larger areas A in the distribution and for small n by the small areas. In some sense $Q_n(\beta,A^*_{n,\beta})$ is a "sensitivity" factor: out of the wide distribution of areas, observation of the nth harmonic selects out only areas near $A^*_{n,\beta}$.

To examine the dependence of $\Delta\alpha$ on the ac field β, we show in Fig. 9(c), $|Q_n(\beta,A)|$ vs A for $n=5$, $\beta=10.0$. The dominant peak, $A^*_{n,\beta}=0.58$, corresponds to dip spacing $\Delta\alpha=5.45$, in good agreement with that computed from Eq. (2a), $\overline{\Delta\alpha}=5.39$. Additional calculation shows that approximately $\Delta\alpha\propto\beta$, i.e., $\Delta H_0\propto H_1$, for large enough values of H_1. We show below that this behavior is observed experimentally.

To summarize, the unexpected observation of sharp, almost periodic dips in the nth harmonic power with dc field for a distribution of loop areas A can be understood semiquantitatively as the consequence of the folding of a rapidly decreasing function $F(A)$ and the rapidly increasing part of the Bessel function $J_n(x)$.

Structure in the intermediate-H_1 region. Figure 10 shows what happens to $P(1\delta f)$ vs H_0 as the ac field is reduced from $H_1=23$ to 2 Oe. The spacing ΔH_0 decreases, initially linearly with H_1, as expected from the argument in the previous paragraph. Then structure develops, which seems irregular, and depends on the sense of the H_0 scan, e.g., Figs. 10(c) and 10(e). However, if the leftward trace is reversed, shown as the dotted line in Fig. 10(d), it superposes exactly on the rightward trace. This is the same property shown by the traces in Fig. 5 and is possibly a consequence of fluxon pinning and depinning,[14] but here the narrow spacing gives an enhanced effect. In Figs. 10(i) and 10(j) there are many resolved and reproducible sharp dips not uniformly spaced but with average spacing still roughly proportional to H_1. This behavior in the intermediate-H_1 region is similar to the flux jumps observed in nonresonant microwave absorption in low fields [see Fig. 15(c)], but is not really understood yet.

A set of $P(nf)$ vs H_0 traces taken as in Fig. 10 but for *odd* harmonics shows similar behavior for large H_1, with ΔH_0 linearly proportional to H_1, but with the dips decreasing in amplitude as H_1 becomes small. The sharp spikes in Figs. 10(i) and 10(j) are not observed for odd

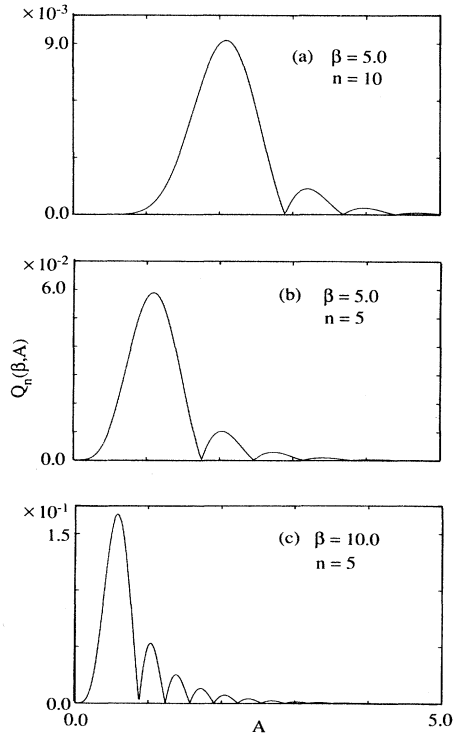

FIG. 9. $|Q_n(\beta,A)|\equiv|AJ_n(A\beta)F(A)|$ vs A, in dimensionless units; $F(A)$ from Eq. (5). (a) $n=10$, $\beta=5.0$; (b) $n=5$, $\beta=5.0$; (c) $n=5$, $\beta=10.0$.

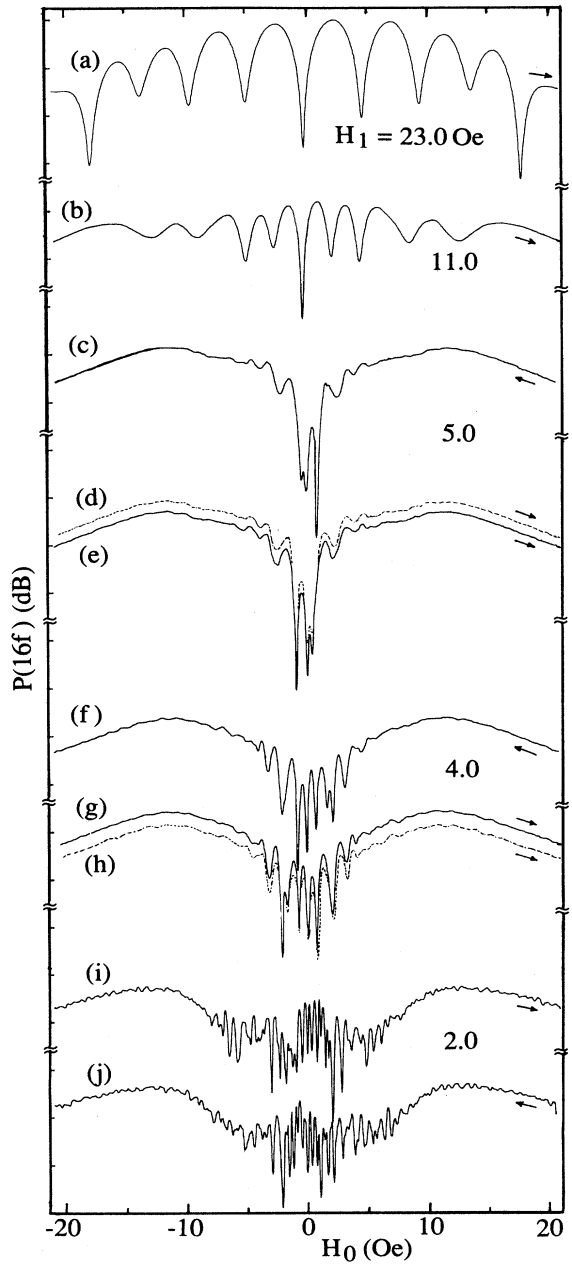

FIG. 10. Relative harmonic power (10 dB/div) $P(16f)$ vs H_0 for sample C-15 powdered Y-Ba-Cu-O at $T=77$ K, $f=28$ kHz, for a series of values of the ac field H_1; the arrows denote the direction of increasing time in the scan. If leftward trace (c) is reversed and plotted (d), it superposes exactly on the rightward trace (e).

harmonics.

Figure 11 summarizes the experimental results in a plot of the values of H_0 for the dips versus the magnitude of H_1. The circles denote positions of well-resolved dips, the diamonds regions of unresolved and more closely spaced dips. The solid lines are plots of the dip positions α versus the ac field β, computed for the zero-order model, Eqs. (2) and (5). This figure shows graphically the general agreement between experiment and theory for large H_1, with poor agreement for $H_1 < 5$ Oe.

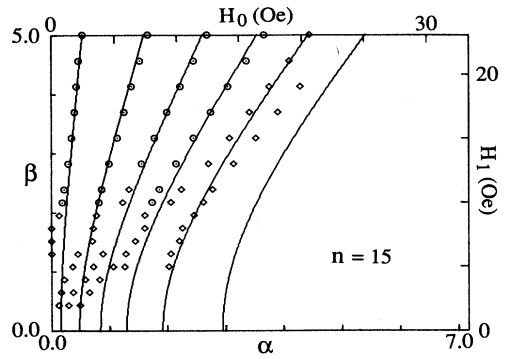

FIG. 11. Circles: Measured values of the dc field H_0 for a sharp dip in $P(15f)$ as a function of the ac field H_1; taken for sample C-15 at 77 K. Diamonds denote less well defined dips. Solid lines: β vs α, where $\alpha \propto H_0$ is the computed position of a sharp dip as a function of $\beta \propto H_1$. Computation is made from Eqs. (2) and (5).

Structure in the second harmonic. The smooth deep narrow dips in $P(nf)$ vs H_0, Fig. 4, are observed only in the high-H_1 region. Figure 12 shows the behavior in the same sample as the ac field is reduced to the intermediate region: at $H_1=1$ Oe the dip has broadened; at $H_1=0.5$ Oe there is a fairly abrupt transition to a wide dip with more hysteresis; at 0.4 the pattern is seen to consist of three dips, which broaden and change shape at 0.2 Oe. Although this structure is not predicted by the zero-order model, we find the loop model does predict similar behavior, shown in Fig. 13, computed from Eqs. (3) and (5). Although this model does not predict the hysteresis, whose origin is noted above, the abrupt onset of the structure is reasonably close to the experimental behavior. We do not yet know if there are alternative explanations, e.g., the onset of a critical state behavior, described below.

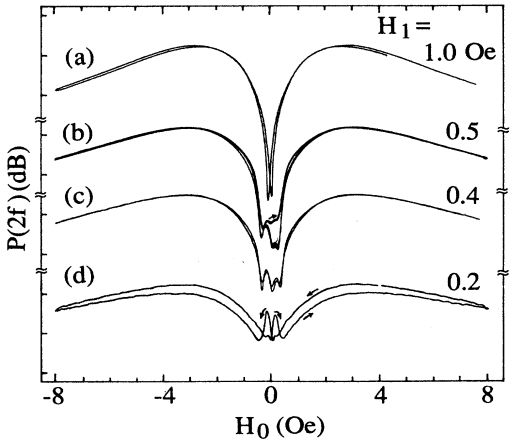

FIG. 12. Relative harmonic power (10 dB/div) for $P(2f)$ vs H_0 for sample C-15, $T=77$ K, showing well-defined transition, with structure, as H_1 field is reduced. Similar behavior is observed for $n=4$.

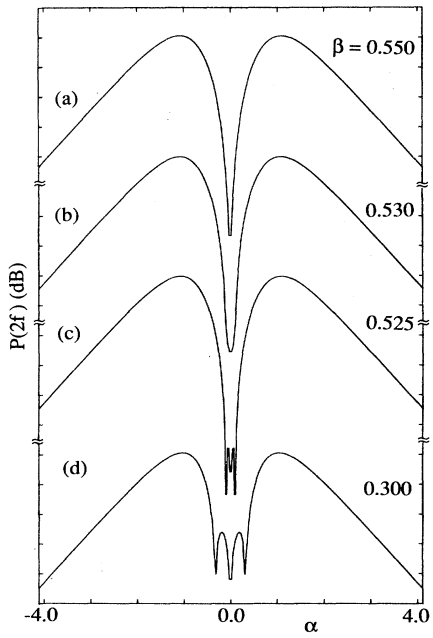

FIG. 13. Relative harmonic power (10 dB/div) for $P(2f)$ vs α, computed from the "loop" model, Eqs. (3) and (5). An abrupt transition to structure is observed as β is reduced; cf. Fig. 12.

Coherent detection of the second harmonic voltage. This transition to low-H_1 behavior was studied by recording the output of the lock-in detector $V_c(2f)$ versus the scanned H_0 field, Fig 14. In Fig. 14(a), $H_1=1$ Oe and we are still roughly in the high-H_1 region; the observed shape is similar to that predicted from Eqs. (2) and (5). A transition has occurred, Fig. 14(b), at $H_1=0.1$ Oe, and the shape has drastically changed, with large hysteresis, more fully developed in Fig. 14(c), at $H_1=0.05$ Oe, with a symmetry and shape similar to that observed for the $M(H)$ hysteresis loop of superconductors in the critical state.[18] Traces of the lock-in voltage for $n=1$, $V_c(1f)$ vs H_0, are symmetric about $H_0=0$, and do not show hysteresis when H_1 is reduced to low values.

Nonresonant microwave absorption[5] has been widely reported and is related to the experiments we report here at much lower frequencies. To demonstrate this we show in Fig. 15 the magnetic-field-modulated derivative of the absorption at $f=9.6$ GHz versus the dc field H_0, for a Y-Ba-Cu-O pellet at $T=14$ K. The field modulation frequency is 8.7 kHz and with amplitude $H_m=5$ Oe in Fig. 15(a), which bears a strong resemblance to Fig. 14(a); they are both in the high-H_1 region. In the intermediate region, Fig. 15(c), $H_m=0.11$ Oe, is to be compared to Fig. 14(b), $H_1=0.1$ Oe. In the low-field region, Fig. 15(d), $H_m=0.03$ Oe, has the symmetry of the critical state, as does Fig. 14(c). Thus the amplitude of modulation H_m in the microwave experiments plays a role similar to the ac amplitude H_1 in the low-frequency experiments, where the frequency f is comparable to the modulation frequency. The striking feature of Figs. 15(d) and 14(c), for small ac fields, is that the sign of the signal voltage depends on the direction of the dc field sweep. This

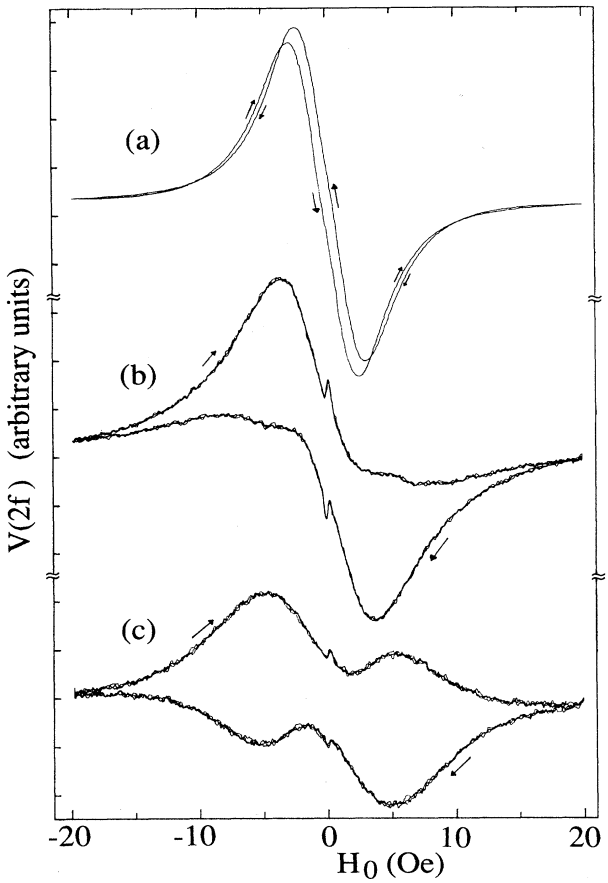

FIG. 14. Relative lock-in detector output voltage $V_c(2f)$ vs H_0 for sample C-15, $T=77$ K, $f=28$ kHz. (a) $H_1=1$ Oe; essentially the same shape is observed at $H_1=5$ Oe; (b) $H_1=0.1$ Oe; (c) $H_1=0.05$ Oe.

phenomenon has been studied by Blazey, Portis, and Bednorz[14] and by Warden *et al.*[19] who show that it is a consequence of fluxon pinning and depinning in the critical state. However, this is greatly reduced [e.g., Figs. 14(a) and 15(a)] for large ac fields, which apply a force exceeding the pinning force.

Linear ac susceptibility. In Sec. II we showed that the normalized lock-in signal for $n=1$ yields the real (χ') and imaginary (χ'') components of the complex ac susceptibility. These were measured, Fig. 16, in zero dc field, as a function of H_1 over 3 orders of magnitude, showing a transition from the high-H_1 to the intermediate- and low-H_1 regions. In Fig. 16(a), made by the two-coil method for powder sample C-15, the vertical axis is proportional to $|4\pi\chi'|$, showing large screening for $H_1 \lesssim 0.1$ Oe, and a transition to greatly reduced screening at $H_1 \gtrsim 10$ Oe. In Figs. 16(b) and 16(c), made by the one-coil method for a pellet sample (C-40), the vertical axes are proportional to $|1+4\pi\chi'|$ and $|4\pi\chi''|$, respectively. The data show at some "large" field $H_1=10$ Oe that $|4\pi\chi'|$ has its minimum value while χ'' is very small, i.e., there is very little ac loss. As H_1 is reduced there is a transition at $H_1 \approx 3$ Oe characterized by a peak in χ'', in the intermediate region. Below $H_1 \approx 0.01$ Oe, χ'' has again dropped to essentially zero and $|4\pi\chi'|$ has reached its

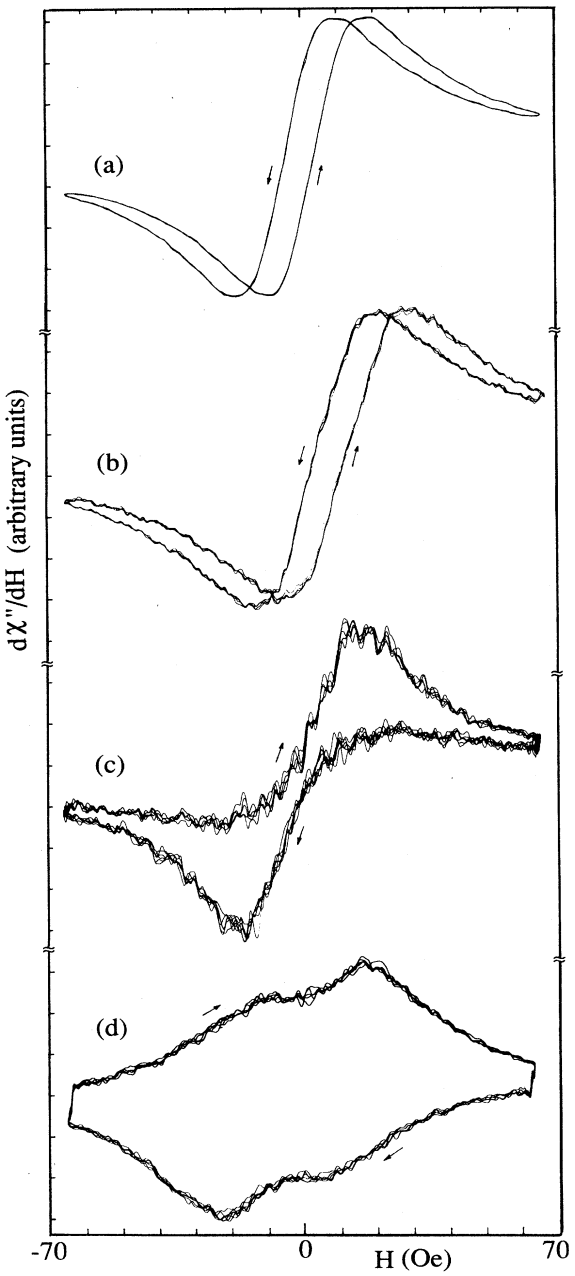

FIG. 15. Nonresonant microwave absorption at $f=9.6$ GHz for Y-Ba-Cu-O pellet at $T=14$ K, using magnetic field modulation $H_m\cos(2\pi f_m t)$, and lock-in detection, with $f_m=8.7$ kHz. (a) $H_m=5.0$ Oe, relative lock-in gain$\equiv 1.0$; (b) $H_m=0.5$ Oe, relative gain$=5$; (c) $H_m=0.11$ Oe, relative gain$=50$; (d) $H_m=0.03$ Oe, relative gain$=50$. Each figure is a superposition of five scans, revealing reproducible dips due to flux jumps.

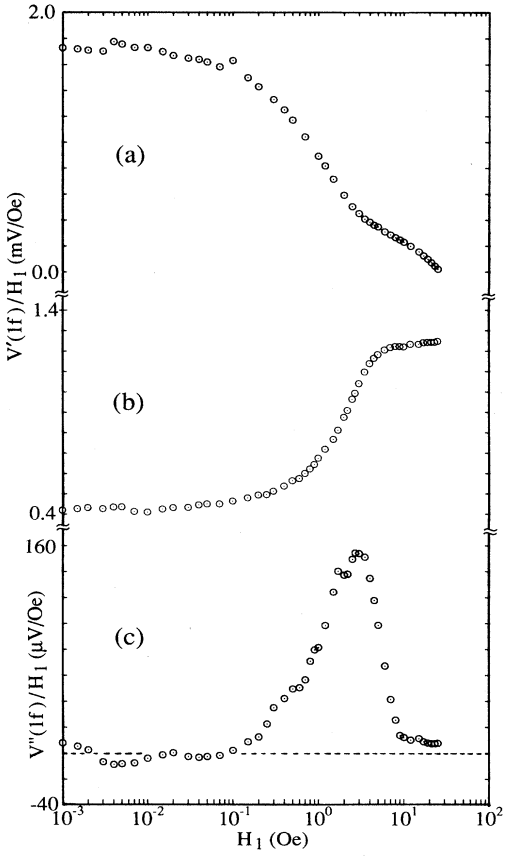

FIG. 16. (a) The inductive phase of the lock-in voltage at the fundamental frequency ($f=28$ kHz), normalized by the ac field H_1, measured by the two-coil method for Y-Ba-Cu-O powder (sample C-15) at $H_0\leq 1$ mOe, $T=77$ K. The vertical axis is just proportional to $|4\pi\chi'|$. (b) Inductive phase of the fundamental lock-in voltage ($f=28$ kHz), normalized by the H_1, measured by the one-coil method for a Y-Ba-Cu-O pellet (sample C-40) at $T=77$ K, $H_0\leq 1$ mOe. The vertical axis is proportional to $|1+4\pi\chi'|$. (c) Same as (b), but resistive phase; vertical axis proportional to $|4\pi\chi''|$; the broken line marks the zero-voltage level.

largest (negative) value. Taking demagnetization effects into account,[20] and finding the demagnetization factor D to be 0.088 for the geometry of sample C-40,[21] the minimum and maximum values for $|4\pi\chi'|$ are calculated to be 0.21 ± 0.03 and 0.85 ± 0.13, respectively. The behavior in Fig. 16(b) is quite similar to that of Raboutou *et al.*,[4] for a Y-Ba-Cu-O pellet at 77 K. Following their ideas as well as those of Clem,[22,23] we draw a simple picture of what is happening in the low-H_1 to high-H_1 transition: At very low H_1 the ac field creates few vortices; χ' is constant. At high H_1, most vortices are freely swept in and out of the sample with the ac field and χ' is again constant. At intermediate fields there is a nonlinear region in which a significant portion of the vortices is being pinned and unpinned by surface or volume pinning centers, giving rise to hysteresis and ac losses. Other loss mechanisms are also possible, e.g., flux flow or "eddy current" losses, which should be frequency dependent.

V. SUMMARY AND CONCLUSIONS

In Sec. III we reviewed several variations of a simple model of granular superconductors that numerically predicts the electrodynamic behavior for bulk materials by

suitably averaging over an area distribution $F(A)$ of flux quantized current loops containing weak links. We have presented a number of experimental data on Y-Ba-Cu-O powder and pellets at 77 K in parallel dc and ac fields, $H=H_0+H_1\sin(2\pi ft)$, for H_0 and H_1 each in the range 0 to 20 Oe, and f in the range 28 to 52 kHz. For a given H_0 the data are sensitive to the magnitude of H_1, and we roughly distinguish these regions: "low-H_1," where presumably fluxons have not penetrated the intergranular space; "intermediate-H_1," where fluxons are being pinned and depinned, with hysteresis and ac loss; and "high-H_1," where most of the fluxons are freely swept in and out of the intergranular space. The models in Sec. III are valid for the high-H_1 region, and do not take account of fluxon motion or pinning. We have not investigated the even higher field region where $H_1 > H_{c1}$ for the grains themselves.

In the high-H_1 region extensive harmonic generation is experimentally observed for all harmonics up to at least $m=41$. If $H_0=0$ the even harmonic power shows a deep (85 dB) and sharp dip, a consequence of the symmetry of Eq. (2b). Remnant local fields from fluxon pinning, together with a tendency for self-symmetry-breaking prevents the even harmonic power from actually dropping below the spectrum analyzer sensitivity (-125 dBm). The odd harmonic power falls off slowly (~ 2 dB/harmonic) and is in fair agreement with the predictions of Eq. (2a) and Eq. (5) for a monotonically decreasing distribution function $F(A)$. This same model also explains the shape of the lock-in signals, $V(f)$ vs H_0 and $V(2f)$ vs H_0 in the high-H_1 region. Gaussian distributions and uniform distributions do not explain the data for our samples for small n.

The temperature dependence of $P(nf)$, $n=2,3,4$, is reasonably consistent with that expected for Josephson junctions; however, the limited temperature range of the data, $77\ \text{K} < T < 95\ \text{K}$, does not preclude other types of weak links.

All versions of the model predict the rather surprising result that for large n the harmonic power should show sharp dips (40 dB) essentially periodic in the dc field (cf. Fig. 6), and this was experimentally verified (cf. Fig. 5) for powder and pellets. This strong evidence of flux quantization is the principal new result of this paper and was observed in many samples of Y-Ba-Cu-O. We argue above in Sec. IV that this structure is a consequence of the product of the (decreasing) distribution function $F(A)$ and the Bessel functions $J_n(A\beta)$ in Eq. (2), and that large areas contribute to high harmonic power generation and vice versa. Except for the small hysteresis in Fig. 5 due to fluxon pinning and depinning, the data of Figs. 1, 2, 4, 5, and 7 can be reasonably understood by the models of Sec. III in the high-H_1 region, perhaps best by Eq. (2) with the distribution function $F(A)$ given by Eq. (5), a monotonically decreasing function obtained empirically. However, we do not claim to have shown that real samples will all be well represented by this function; in fact, even for the samples reported here, more work on refining $F(A)$ will be needed to fit the data more quantitatively.

As H_1 is reduced new phenomena appear as in Fig. 12, showing onset of additional fine structure in the dips for $n=2,4,\ldots$. This behavior is predicted by the loop model, Eqs. (3) and (5), in Fig. 13, which could represent flux quantized loops without weak links; this is experimentally possible since details of the sample microstructure are not known. However, other mechanisms cannot yet be ruled out, e.g., onset of a critical state. For example, under the same conditions as Fig. 12, the lock-in detected second harmonic signal at 56 kHz, Fig. 14, shows a transition to the intermediate and low-H_1 regions as H_1 is further reduced. In fact, the behavior in Fig. 14 is remarkably similar to the lock-in signals from modulated microwave absorption, Fig. 15, showing transition to a critical state in Fig. 15(d).

From the measurement of the complex ac susceptibility χ' and χ'', Fig. 16, one can see more directly the transitions from high-H_1 behavior (small shielding, small loss) to the intermediate region (maximum ac hysteresis loss), to the low-H_1 region (maximum shielding, low loss).

Clearly much remains to be done to understand the complex and interesting problem of the electrodynamics of granular superconductors. The microscopic models presented here are *sufficient* to explain much of our data at large H_1, but we have yet to show that they are also *necessary*; simple emperical or phenomenological models may also suffice. Data over a wider range of temperature, frequency, magnitude, and orientation of the ac and dc fields will be essential, and are in progress. Although the experimental phenomena we report here are believed to be generic to Y-Ba-Cu-O, and probably also to $Bi_4Sr_3Ca_3Cu_4O_x$,[9] similar studies of other materials, including films, single crystals, powders, and pellets with different grain sizes and methods of preparation, are also essential and may reveal additional phenomena. The theoretical models of Sec. III should be generalized to include the geometry of the sample, the critical state, and fluxon pinning and motion. Finally, we note that some interesting work on harmonic generation by Y-Ba-Cu-O has also been done by Shaulov and Dorman.[24] However, they were interested in the very small H_1 regime, as first suggested by Bean on conventional type-II superconductors,[18] in contrast to what we have mainly reported in this paper.

ACKNOWLEDGMENTS

We are indebted to Professor John Clarke for his insights and suggestions in modeling the problem. We would also like to thank Professor A. M. Portis for a careful reading of the manuscript with very useful comments. We also thank Dr. J. P. Crutchfield, Dr. A. Behrooz, Dr. L. C. Bourne, Dr. M. Hundley, Dr. D. Britt, and Dr. F. Wellstood for helpful discussions. This work was supported in part by the Director, Office of Energy Research, Office of Basic Energy Sciences, Materials Sciences Division of the U.S. Department of Energy under Contact No. DE-AC03-76SF00098; the Office of Naval Research under Contract No. N00014-86-K-0154; and by the National Science Foundation under Grant No. DMR-84-00041.

[1]K. A. Müller, M. Takashige, and J. G. Bednorz, Phys. Rev. Lett. **58**, 1143 (1987); F. S. Razavi, F. P. Koffyberg, and B. Mitrovic, Phys. Rev. B **35**, 5323 (1987).
[2]C. Ebner and D. Stroud, Phys. Rev. B **31**, 165 (1985).
[3]R. B Goldfarb *et al.*, Cryogenics **27**, 475 (1987).
[4]A. Raboutou *et al.*, Europhys. Lett. **4**, 1321 (1987).
[5]K. W. Blazey *et al.*, Phys. Rev. B **36**, 7241 (1987); K. Khachaturyan *et al.*, *ibid.* **36**, 8309 (1987); D. Durny *et al.*, *ibid.* **36**, 2361 (1987); E. J. Pakulis *et al.*, Physica C **153–155**, 510 (1988); S. H. Glarum, J. H. Marshall, and L. F. Schneemeyer, Phys. Rev. B **37**, 7491 (1988).
[6]J. F. Kwak *et al.*, in *Proceedings of the International Workshop on Novel Mechanisms of Superconductivity, Berkeley, 1987,* edited by S. A. Wolf and V. Z. Kresin (Plenum, New York, 1987), p. 983; R. L. Peterson and J. W. Ekin, Phys. Rev. B **37**, 9848 (1988).
[7]C. D. Jeffries *et al.*, Phys. Rev. B **37**, 9840 (1988).
[8]Q. H. Lam and C. D. Jeffries, Phys. Rev. B **39**, 4772 (1989).
[9]Q. H. Lam, C. D. Jeffries, A. Behrooz, P. Pinsukanjana, and A. Zettl (unpublished).
[10]Same sample used in Ref. 7; preparation procedure described in L. C. Bourne *et al.*, Phys. Lett. A **120**, 494 (1987). Briefly, the sample preparation was: Grind together stochiometric mixture of Y_2O_3, $BaCO_3$, and CuO in acetone in ball grinder; calcinate in O_2 at 700 °C for 6 h, regrind and recalcinate; press into cylindrical pellets at ~7000 psi in stainless-steel cylinder; heat at 950 °C for ~30 h in O_2 and cool slowly (950 °C→ 400 °C in 10 h); resistive measurement of transition temperature of pellet yields T_c =91 K; grind pellet to powder in agate mortar. Optical microscopic examination of powder showed shiny chunks ranging in size between 10 to 1 μm (limit of resolution).
[11]Sample provided by Colorado Superconductor Inc.
[12]T. Xia and D. Stroud, Phys. Rev. B **39**, 4792 (1989).
[13]V. Ambegaokar and A. Baratoff, Phys. Rev. Lett. **10**, 486 (1963); **11**, 104(E) (1963).
[14]See, for example, K. W. Blazey, A. M. Portis, and J. G. Bednorz, Solid State Commun. **65**, 1153 (1988), and references therein.
[15]M. E. McHenry *et al.*, Phys. Rev. B **37**, 623 (1988).
[16]B. Jeanneret, Ch. Leemann, and P. Martinoli, Jpn. J. Appl. Phys. **26**, Suppl 26-3, 1417 (1987). Also see A. Behrooz *et al.*, Phys. Rev. Lett. **57**, 368 (1986) for the case of quasicrystalline superconducting networks.
[17]R. A. Webb *et al.*, Phys. Rev. Lett. **51**, 690 (1983); Ch. Leemann *et al.*, *ibid.* **56**, 1291 (1986); M. Tinkham, D. W. Abraham, and C. J. Lobb, Phys. Rev. B **28**, 6578 (1983).
[18]C. P. Bean, Rev. Mod. Phys. **36**, 31 (1964); P. W. Anderson, Phys. Rev. Lett. **9**, 309 (1962).
[19]M. Warden *et al.*, J. Appl. Phys. **64**, 5800 (1988), and references therein.
[20]S. D. Murphy *et al.*, Solid State Commun. **69**, 367 (1989).
[21]R. B Goldfarb and J. V. Minervini, Rev. Sci. Instrum. **55**, 761 (1984).
[22]J. R. Clem, Ames Laboratory, Ames, Iowa, Tech. Report No. IS-M280, 1980 (unpublished).
[23]J. R. Clem, Physica C **153–155**, 50 (1988).
[24]A. Shaulov and D. Dorman, Appl Phys. Lett. **53**, 2680 (1988). We are grateful to A. M. Portis for bringing this paper to our attention.